Reaction Chemistry & Engineering

ROYAL SOCIETY OF CHEMISTRY

PAPER

Cite this: *React. Chem. Eng.*, 2023, **8**, 3071

Synergetic effects of a poly-tartrazine/CTAB modified carbon paste electrode sensor towards simultaneous and interference-free determination of benzenediol isomers†

Amit B. Teradale, [a] Kailash S. Chadchan, [b] Pattan-Siddappa Ganesh,[c] Swastika N. Das *[b] and Eno E. Ebenso[de]

Dihydroxybenzene (DHB) isomers like catechol (CC), hydroquinone (HQ), and resorcinol (RC) pose a significant threat to human health and the environment due to their persistence and ability to cause harm to vital organs. Detecting these chemicals can be challenging because they have similar properties and structures, and they coexist in the environment. This study introduces a novel approach in the field by developing a modified carbon paste electrode called poly-tartrazine/cetyl trimethyl ammonium bromide/modified carbon paste electrode (poly-TZ/CTAB/MCPE). The electrode was created by polymerizing tartrazine (TZ) onto the carbon paste electrode (CPE) surface, followed by the application of cetyl trimethyl ammonium bromide (CTAB) solution. The incorporation of TZ and CTAB onto the CPE surface resulted in enhanced sensitivity for detecting dihydroxy benzene isomers. By utilizing cyclic voltammetry (CV) and differential pulse voltammetry (DPV) techniques, our modified electrode successfully detected and distinguished each of the three isomers individually and simultaneously. The peaks obtained were well-defined, and there were adequate potential differences between each peak. The detection limits for CC, HQ and RC were found to be 0.495×10^{-6} M, 0.41×10^{-6} M and 2.2×10^{-6} M, respectively. This modified electrode exhibited selectivity, reproducibility, and repeatability properties. Unlike previous research, our study delves into the combined interactions between CTAB and tartrazine, specifically with the dihydroxy benzene isomers.

Received 7th June 2023,
Accepted 10th August 2023

DOI: 10.1039/d3re00318c

rsc.li/reaction-engineering

1. Introduction

o-Benzenediol (catechol), *p*-benzenediol (hydroquinone), and *m*-benzenediol (resorcinol) are three dihydroxybenzene positional isomers (Scheme S1†) that are widely used as intermediate products in various fields, including organic synthesis, dyestuffs, pesticides, flavoring agents, secondary coloring compounds, photography chemicals, cosmetics, and medicine. However, during their production and use, these isomers are often unintentionally released into the environment, causing contamination of rivers and groundwater. One of the most significant challenges in dealing with these compounds is their persistence in aquatic environments, making them difficult to degrade. This persistence can pose a significant risk to the ecosystem and its living organisms, including humans, even at low concentrations. For instance, prolonged exposure to CC and HQ can lead to accelerated damage to the human body's neural system, kidneys, and skin tissue. These hazards have been well-documented in scientific research. Moreover, these isomers are structurally and chemically similar, making their simultaneous determination a significant challenge. The coexistence of these compounds further complicates their detection, highlighting the need for advanced analytical techniques to differentiate and quantify them accurately. In conclusion, monitoring these hazardous dihydroxybenzene positional isomers in the environment is essential to protect the health of the ecosystem and human beings.[1–4]

A variety of analytical methods have been employed to identify the isomers of dihydroxy benzenes, including HPLC,[5–7] chemiluminescence,[8] spectrophotometry,[9]

[a] *PG Department of Chemistry, BLDEA's S.B. Arts and K.C.P. Science College, Vijayapur, Karnataka, 586103, India*
[b] *Department of Chemistry, BLDEA's V. P. Dr. P. G. Halakatti College of Engineering and Technology, Vijayapur-586103, Karnataka, India. E-mail: drswastika@yahoo.com; Fax: +8352 262945; Tel: +8352 261120*
[c] *Advanced Technology Research Center, Korea University of Technology and Education, Cheonan-si, Chungcheongnam-do, 31253, Republic of Korea*
[d] *Centre for Material Science, College of Science, Engineering and Technology, University of South Africa, Johannesburg 1710, South Africa*
[e] *Institute of Nanotechnology and Water Sustainability, College of Science, Engineering and Technology, University of South Africa, Johannesburg 1710, South Africa*

† Electronic supplementary information (ESI) available. See DOI: https://doi.org/10.1039/d3re00318c

fluorescence,[10] and gas chromatography/mass spectrometry.[11] Despite their usefulness, these methods suffer from several drawbacks such as high cost, time-consuming procedures, unsuitability for on-site analysis, and the need for skilled operators and complex instruments. To address these challenges and detect trace levels of dihydroxy benzene isomers more efficiently, voltammetric methods have garnered increasing attention due to their numerous advantages including low cost, rapid response, simplicity, high sensitivity, accuracy, and repeatability.[12–14] Additionally, electrochemical sensors are well-suited for simultaneously detecting multiple analytes and on-site detection, and can be integrated with robust, portable, or miniaturized devices for targeted experiments in clinical and diagnostic applications.[15–20]

Electrode modification is a key area of interest, enabling the alteration of electrochemical properties using various materials. Modified electrodes have shown promise in detecting substances at low concentrations.[21–26] The functionality of modified electrodes depends on the specific characteristics of the applied modifier during the modification process.[27,28] Modified electrodes can enhance sensitivity for detecting biological specimens and medicines at very low concentrations (macro to nanomolar level) in biomedical research and pharmaceutical applications.[29–31] Various electrochemical methods are used to detect CC and HQ simultaneously which remained a topic of interest for the researchers due to the overlap in their redox peaks at bare electrode surfaces.[2–4,32–38] While some electrochemical methods can detect catechol and hydroquinone together, few studies focus on simultaneously detecting catechol, resorcinol, and hydroquinone. Recent research has explored new electrode materials for this purpose,[39–45] but further innovation is sought. In the present work, we have tried to develop a modified carbon paste electrode (CPE) as it has gained significant importance due to its various advantages reported in several articles.[46,47] Synthetic dyes are used to develop biosensors to detect various organic molecules, and several such reports are available.[48–52] In the present work, an azo dye, tartrazine, was selected as a sensing substance for the carbon paste electrode due to its stability, low cost, and the presence of an azo group in its molecular structure. Further, a cationic surfactant, CTAB, was immobilized on the tartrazine–carbon paste surface for better bonding of the dye onto the surface, enhancing the stability of the sensor. The combined interactions of CTAB and tartrazine with dihydroxy benzene isomers make this study attractive. The newly developed sensor is suitable for the simultaneous and interference-free determination of benzenediol isomers. To the best of our knowledge, this synergistic effect has not been explored in previous studies, making our findings both compelling and highly relevant for the scientific community. Our study contributes not only to an enhanced understanding of electrochemical sensing but also opens new possibilities for accurate and selective detection of important compounds like dihydroxy benzene isomers. The potential applications of our innovative sensor design hold great promise in various fields, including environmental monitoring, biomedical research, and pharmaceutical analysis.

2. Experimental section

2.1. Apparatus

Using a CH electrochemical workstation (model CHI-619E), the electro-analytical procedures of CV and DPV were carried out. A saturated calomel electrode (SCE), a platinum wire, and either a bare carbon paste electrode (BCPE) or a modified carbon paste electrode (poly-TZ/CTAB/MCPE) were the three electrodes in the system. All analytes' oxidation potentials were determined at 25 ± 0.5 °C and reported against SCE.

2.2. Reagents and materials

Catechol, hydroquinone, and resorcinol were obtained from Sigma Aldrich Ltd, Tartrazine dye, CTAB surfactant, $NaH_2PO_4{\cdot}H_2O$ and Na_2HPO_4 were purchased from Himedia Pvt. Ltd. Graphite powder and silicone oil were obtained from Loba Chemie. Aqueous stock solutions of CC, HQ, and RC ([CC] = 10×10^{-4} M, [HQ] = 10×10^{-4} M and [RC] = 10×10^{-4} M) were prepared by dissolving necessary amounts of each chemical. An aqueous stock solution of CTAB ([CTAB] = 10×10^{-3} M) was also prepared in a similar way. The solutions of the desired pH were obtained by mixing $NaH_2PO_4{\cdot}H_2O$ and Na_2HPO_4 solutions in an appropriate ratio.

2.3. Preparation of working electrodes (BCPE and MCPE)

The carbon paste electrodes were made by mixing graphite powder and silicone oil in 70 : 30 (w/w) proportions for about thirty minutes until an even paste was obtained. A Teflon tube cavity with an interior diameter of 3 mm was filled in with the paste and connected to an electrical contact. Before each measurement, the carbon paste electrode was polished using tissue paper to achieve a flat, even surface. For each measurement, the paste was gently taken out and refilled. The poly (tartrazine) MCPE was generated by electro-polymerizing 1.0 mM tartrazine in 0.2 M PBS at pH 7.4 using the CV technique.[52]

3. Results and discussion

3.1. Development of the poly-tartrazine modified carbon paste electrode *via* electro polymerization

This research focuses on fabricating a modified carbon paste electrode (MCPE) using electro-polymerization. To achieve this, the BCPE was immersed in a solution containing 1 mM tartrazine, buffered with 0.2 M PBS at a pH level of 7.4. Several potential sweeps ranging from −0.5 V to 2.0 V, with a scan rate of 0.1 V s^{-1}, were applied. The number of cycles was optimized to obtain a stable cyclic voltammogram, with the most effective result observed at ten cycles. A comparison with 5, 15, 20, and 25 cycles showed that 10 potential sweeps produced a more productive modifier. After these 10 cycles, the voltammograms exhibited nearly constant growth indicating the development and stabilization of a durable polymer film on the BCPE, as illustrated in Fig. 1A.

3.2. Development of the CTAB immobilized tartrazine-modified carbon paste electrode

In developing a CTAB-incorporating tartrazine-MCPE, varying concentrations of CTAB solution were adhered to the surface of the modified electrode, as depicted in Fig. 1B. Modifying the electrode with different concentrations of CTAB resulted in different peak current responses for the oxidations of CC, HQ, and RC in 0.2 M PBS at pH 7.4 with a maximum of 4.0 μL of CTAB. Beyond this concentration, any further increase in CTAB concentration leads to a decline in the response. Consequently, 4.0 μL of CTAB solution was selected and left to permeate the porous modified carbon paste electrode at room temperature for roughly 10 minutes. Subsequently, the electrode was cleaned meticulously with double-distilled water to eliminate any extra CTAB adhering to the surface. The final CTAB-enhanced tartrazine-modified CPE exhibited the expected characteristics of a mediator-based sensor, showing an improved electrocatalytic response towards CC, HQ and RC[53] (Scheme S2†).

3.3. Cyclic voltammetric behavior of CC at different modifiers

In this study, the effectiveness of various modified electrodes, namely poly (tartrazine)/CTAB, CTAB-immobilized MCPE, and poly (tartrazine) MCPE with BCPE, was compared for the electrochemical behavior of CC (catechol) using the cyclic voltammetry (CV) technique (Fig. 1C). The CV analysis revealed that both the BCPE (curve a) and CTAB-immobilized BCPE (curve b) did not exhibit significant cyclic voltammetric signals for CC sensing, indicating that CTAB is not highly electrochemically active in detecting CC.

Conversely, a clear anodic peak at around 0.235 V was observed for CC at the poly-tartrazine MCPE without CTAB (curve c). Interestingly, when 4.0 μM CTAB was introduced to the poly-tartrazine MCPE surface, the oxidation peak current of CC increased significantly (curve d). This suggests that CTAB facilitates electron transfer of CC more efficiently in the presence of tartrazine. The enhanced efficiency is likely attributed to the formation of a hydrophilic layer with positive charges on the electrode surface in the presence of CTAB. This hydrophilic layer promotes the easy interaction of CC, leading to an increased concentration of CC at the electrode surface.

3.4. Electrochemical assessment of the poly-TZ/CTAB/MCPE sensor using standard $K_4Fe(CN)_6$solution

In conventional cyclic voltammetric studies, the electrochemical assessment of the newly modified electrode uses a standard solution of $K_4Fe(CN)_6$ in 1.0 M KCl electrolyte, as a redox probe.[54] Accordingly, the newly fabricated poly-TZ/CTAB/MCPE sensor was used to investigate the same redox probe

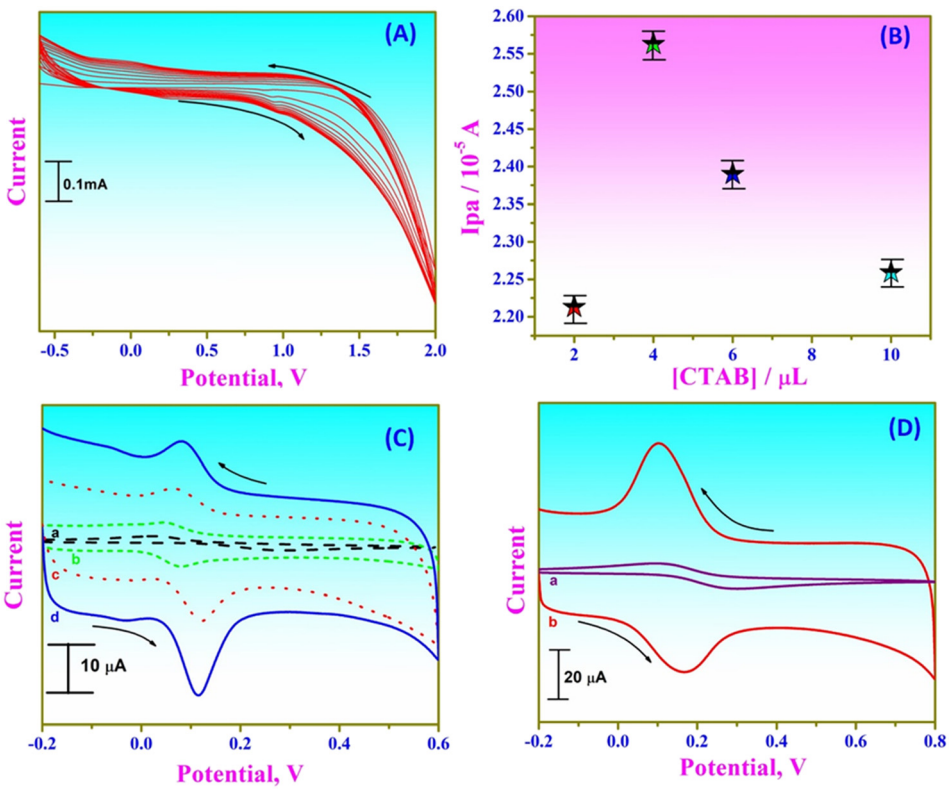

Fig. 1 (A) Polymerization of TZ on BCPE with ten multiple cycles with a scan rate of 0.1 V s^{-1} by the CV technique. (B) Plot displaying the different anodic peak currents obtained with varying concentrations of CTAB immobilized on poly-TZ/MCPE during the oxidation of 0.1 mM CC in 0.2 M PBS at pH 7.4. (C) Different CV curves for CC at different MCPEs: (a) at bare CPE; (b) CPE + CTAB; (c) CPE + TZ; (d) CPE + TZ + CTAB. (D) Reversible CV curves of the $[Fe(CN)_6]^{2+}/[Fe(CN)_6]^{3+}$ probe at bare CPE (-----) and poly-TZ/CTAB/MCPE (—), with a scan rate of 0.05 V s^{-1}.

using the CV technique. The cyclic voltammogram was acquired within a potential range of −0.2 to 1.0 V at a scan rate of 0.05 V s^{-1}, as demonstrated in Fig. 1D. The assessment elucidated that the bare CPE (indicated by the dashed line in the figure) provided a limited sensitivity due to the sluggish rate of the electron transfer reaction. Conversely, the poly-TZ/CTAB/MCPE sensor (represented by the figure's solid line) showed substantial improvement in electron transfer kinetics and reproducibility under identical conditions. This result affirms that the surface characteristics of the BCPE have undergone significant modifications in the presence of tartrazine-CTAB, resulting in boosted electrocatalytic activity. The observed ΔEp value was found to be in line with the characteristic reversible cyclic voltammogram of the $[Fe(CN)_6]^{2+}$/$[Fe(CN)_6]^{3+}$ probe.

The total active surface area was calculated using the standard Randles–Sevcik equation (eqn (1)).[55]

$$Ip = 2.69 \times 10^5 n^{3/2} A D^{1/2} C_0 v^{1/2} \quad (1)$$

The peak current (Ip) is influenced by factors such as the concentration of the electroactive species (C_0), the number of electrons (n), the diffusion coefficient (D), the scan rate (v), and the electroactive surface area (A). When considering the poly-TZ/CTAB/MCPE, the electroactive surface area was higher (0.0338 cm^2) when compared to the bare CPE (0.0146 cm^2). This observation aligns with previous findings.[51–53]

3.5. Electro-oxidation of CC at the poly-TZ/CTAB/MCPE

The electro-oxidation of CC at the poly-TZ/CTAB/MCPE and BCPE was investigated using the CV technique at pH 7.4 with a scan rate of 0.05 V s^{-1} (Fig. 2A). The results revealed that the modified electrode surface exhibited a better voltammetric response compared to the BCPE. The oxidation peak potentials were observed at 0.2947 V and 0.1815 V for the BCPE (dashed line) and poly-TZ/CTAB/MCPE (solid line), respectively. The reduction in the oxidation peak potential or the reduction in overvoltage at the poly-TZ/CTAB/MCPE surface indicated excellent electrocatalytic activity and reproducibility for the electrochemical oxidation of CC.

3.6. The effect of scan rate variation on the peak current of CC at the poly-TZ/CTAB/MCPE

To better understand the reaction kinetics at the electrode–solvent interfaces, the impact of the scan rate variation on the peak current of CC at the poly-TZ/CTAB/MCPE was examined using cyclic voltammetry analysis. The study entailed altering the scan rate within the range of 0.02 to 0.4 V s^{-1} at the poly-TZ/CTAB/MCPE for 0.1 mM CC in 0.2 M PBS with a pH of 7.4 as illustrated in Fig. 2B. An increase in the scan rate led to an escalation in the redox peak currents, accompanied by a minor shift in the redox peak potentials. A plot of peak currents (Ip) against scan rates (v) demonstrated excellent linearity with correlation coefficients of 0.9996 (Ipa) and

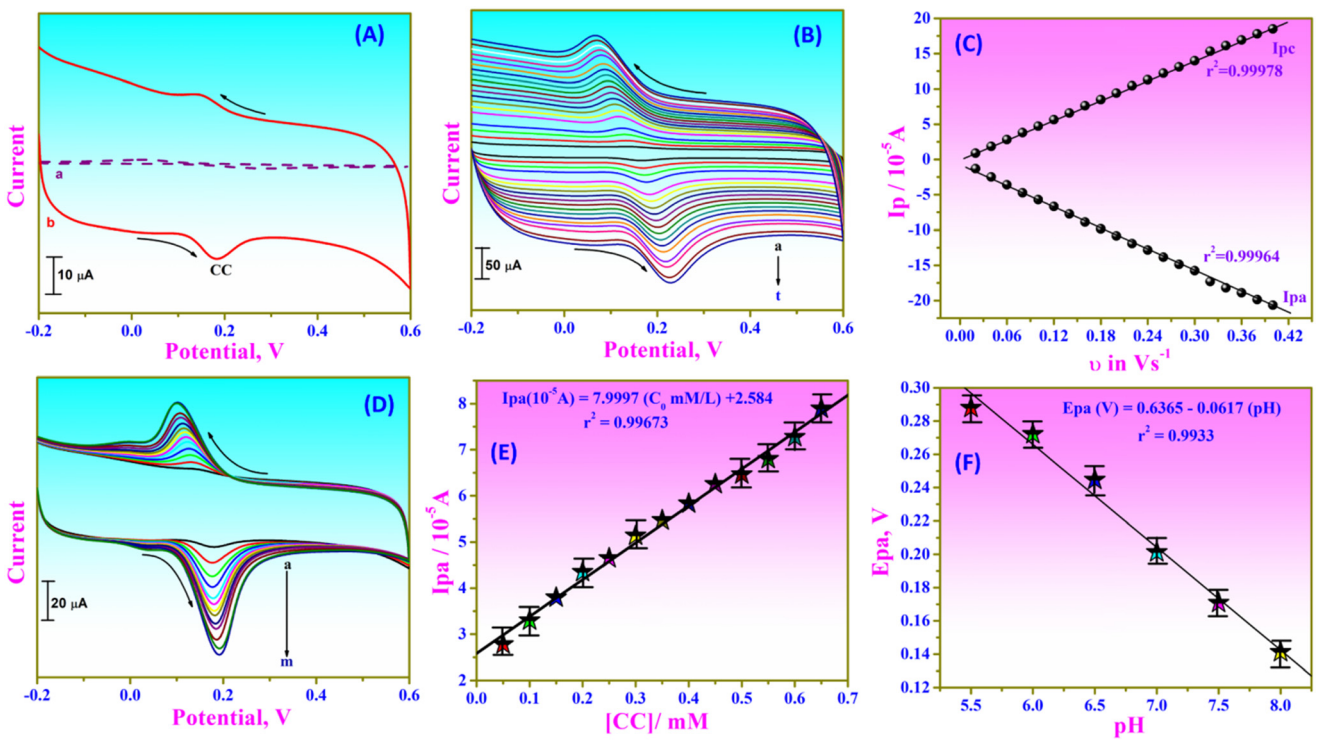

Fig. 2 (A) The CV curves for 0.1 mM CC at BCPE (-----) and poly-TZ/CTAB/MCPE (—) in 0.2 M PBS of pH 7.4 at a scan rate of 0.05 V s^{-1}. (B) The CV curves for 0.1 mM CC at poly-TZ/CTAB/MCPE at different scan rates (a–t; 0.02 V s^{-1} to 0.4 V s^{-1} at an increment of 0.02 V s^{-1}), in pH 7.4 buffer solution. (C) Plot of Ipa *versus* v for CC. (D) Variation of concentration of CC at poly-TZ/CTAB/MCPE (a–m: 0.05 mM to 0.65 mM at an increment of 0.05 M). (E) Plot of Ipa *vs.* concentration of CC. (F) Plot of Epa *vs.* pH.

0.9997 (Ipc), as presented in Fig. 2C. Furthermore, the graph depicting Ip against the square root of the scan rate ($v^{1/2}$), as illustrated in Fig. S1,† revealed correlation coefficients of 0.9879 (Ipa) and 0.9868 (Ipc). This observation advocates that the electrode process is governed by adsorption.[53]

3.7. The effect of CC concentration variation at the poly-TZ/CTAB/MCPE

Cyclic voltammetry was utilized to investigate the electrocatalytic oxidation of CC at the poly-TZ/CTAB/MCPE when the concentration of CC was varied from 0.05 mM to 0.65 mM maintaining the pH of the solutions at 7.4. The cyclic voltammograms corresponding to various concentrations of CC are presented in Fig. 2D. It was noticed that the Ipa value was raised gradually with the rise in the concentration of CC. The following linear regression equation (eqn (2)) could be derived from the Ipa graph (Fig. 2E) against CC concentration.

$$\text{Ipa}(10^{-5}\ \text{A}) = 7.9997\ \text{Co (mM)} + 2.584 \quad (2)$$

The correlation coefficient 0.99673 (Fig. 2E) implies that the Ipa rises with the increase in CC concentration. These findings corroborate earlier published studies.[51,52] The LOD for CC at the poly-TZ/CTAB/MCPE was determined to be 0.49 × 10^{-6} M. For comparison, the detection limits for CC at various modified electrode surfaces are documented in Table 2. The method implemented in this study was more effective than other documented methods.[35,52,56–69]

3.8. The effect of pH variation for the determination of CC at the poly-TZ/CTAB/MCPE

The effect of pH (range of 5.5 to 8.0) on the analysis of CC at the poly-TZ/CTAB/MCPE was investigated using cyclic voltammetry (Fig. S2†). The results indicated that the oxidation peak potential shifted toward a more positive direction with increasing the pH of the solution. The graph of Epa *versus* pH yielded a linear equation of Epa (V) = 0.6365–0.0617 (pH) (Fig. 2F), with a correlation coefficient of 0.9933, suggesting that the electro-oxidation mechanism involves an equal number of protons and electrons, which is consistent with previously reported findings.[50]

3.9. Electrocatalytic oxidation of HQ at the poly-TZ/CTAB/MCPE

A study on the electrocatalytic oxidation of 0.1 mM HQ in 0.2 M PBS of pH 7.4 was carried out using cyclic voltammetry. The voltammograms at the BCPE (represented by the dashed line) and poly-TZ/CTAB/MCPE (represented by the solid line) were recorded. It can be seen from Fig. 3A that the voltammetric response of HQ at the BCPE was of low sensitivity, with the anodic peak potential located at 0.1561 V. In contrast, the oxidation peak potential of HQ at the poly-TZ/

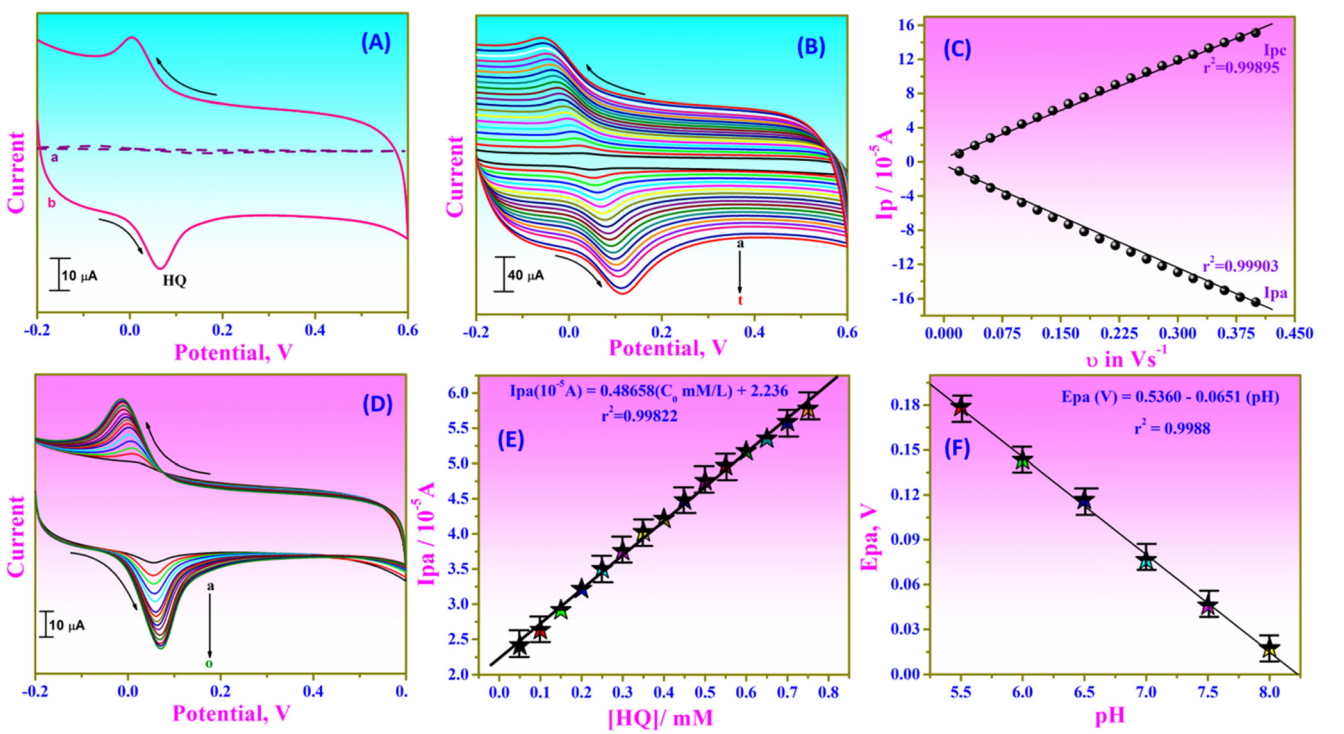

Fig. 3 (A) The CV curves for 0.1 mM HQ at BCPE (-----) and poly-TZ/CTAB/MCPE (—) in 0.2 M PBS of pH 7.4 at a scan rate of 0.05 V s^{-1}. (B) The CV curves for 0.1 mM HQ at the poly-TZ/CTAB/MCPE at different scan rates (a–t; 0.02 V s^{-1} to 0.4 V s^{-1} at an increment of 0.02 V s^{-1}). (C) Plot of Ip *versus* v for HQ. (D) Variation of concentration of HQ at the poly-TZ/CTAB/MCPE (a–o: 0.05 mM to 0.75 mM, at the increment of 0.05 mM). (E) Plot of Ipa *vs.* concentration of [HQ]. (F) Plot of Epa *vs.* pH for HQ.

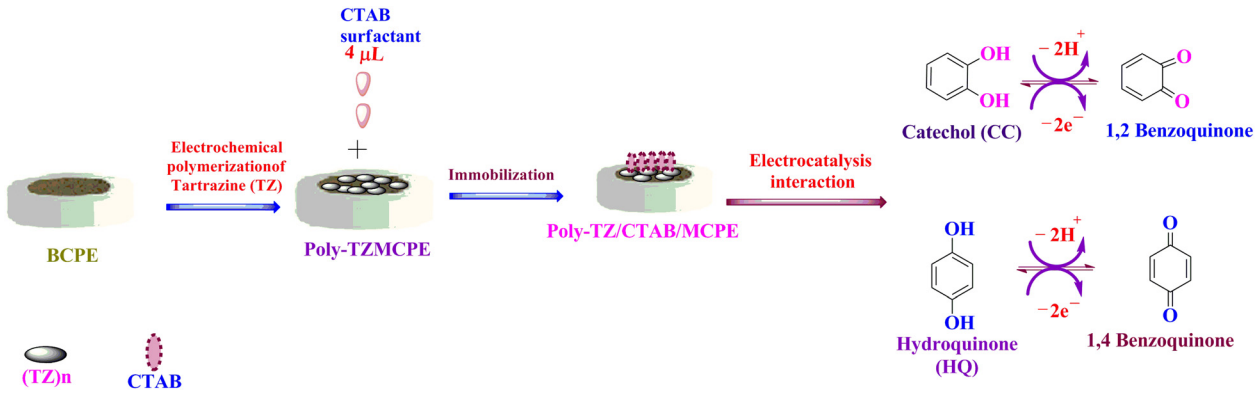

Scheme 1 Probable oxidation mechanism of CC and HQ on the poly-TZ/CTAB/MCPE.

CTAB/MCPE was observed at 0.0655 V, with enhanced peak current indicating better sensitivity of the newly developed poly-TZ/CTAB/MCPE. Scheme 1 illustrates the oxidation mechanisms of CC and HQ.[51,52] The electro-oxidations of HQ at different electrode surfaces are shown in Fig. S3.†

3.10. The effect of scan rate variation on the peak current of HQ at the poly-TZ/CTAB/MCPE

In order to investigate how the peak current of HQ at the poly-TZ/CTAB/MCPE was affected by the scan rate, cyclic voltammetry was performed with varying scan rates ranging from 0.02 to 0.4 V s^{-1} for 0.1 mM HQ in 0.2 M PBS of pH 7.4 as depicted in Fig. 3B. The results showed a proportional relationship between the applied scan rate and the redox peak current. Additionally, there was a slight shift in the anodic and cathodic peak potentials towards more positive and less negative values, respectively. These data were used to generate two graphs: Ip *versus* v (Fig. 3C) and Ip *versus* $v^{1/2}$(Fig. S4†), with the linear correlation coefficient being more significant for the former graph, suggesting that adsorption controls the electrode phenomenon.[51] Further, using eqn (3), the values of the heterogeneous rate constant (k^0) for the CC and HQ oxidations were calculated from the experimental peak potential difference (ΔEp) data for voltammograms with ΔEp values greater than 10 mV.[52] The results of these calculations are presented in an organized manner in Table 1.

$$\Delta Ep = 201.39 \log(v/k^0) - 301.78 \quad (3)$$

To investigate the electrocatalytic oxidation behavior of HQ at the poly-TZ/CTAB/MCPE, the concentration of HQ was varied from 0.05 mM to 0.75 mM. Cyclic voltammograms were recorded, as presented in Fig. 3D. The data revealed a direct correlation between the anodic peak current (Ipa) and the concentration of HQ, as illustrated in Fig. 3E. The linear regression equation for this correlation was determined to

Table 1 Variation of the voltammetric parameters for the scan rate variations of CC and HQ

v/V s^{-1}	Catechol (CC)		Hydroquinone (HQ)	
	ΔEp/mV	k^0/s^{-1}	ΔEp/mV	k^0/s^{-1}
20	27.5	0.4634	29.6	0.4525
40	34.5	0.8556	33.5	0.8655
60	43.2	0.8605	44.2	1.1488
80	51.2	0.7074	55.2	1.3507
100	59.1	0.6192	63.1	1.5424
120	63.9	0.5452	66.9	1.7725
140	72.9	0.5179	62.1	2.1844
160	81.7	1.995	65.0	2.4150
180	89.5	2.053	64.1	2.7452
200	95.5	2.1302	62.1	3.120
220	102.4	2.1653	64.1	3.3552
240	106.3	2.2589	63.2	3.6975
260	116.1	2.1881	63.1	4.0102
280	122.1	2.2001	61.1	4.4193
300	128.9	2.1808	58.1	4.9002
320	136.9	2.123	60.2	5.1021
340	142.6	2.1133	58.1	5.5536
360	147.6	2.1135	57.2	5.9402
380	151.5	2.1334	54.2	6.4890
400	161.4	2.005	56.2	6.6766

Table 2 Comparison of detection limits for CC and HQ with different classical methods and electrodes

Working electrodes	Methods	Limit of detection (μM)		Ref.
		CC	HQ	
Poly-NB/MGCE	CV	0.068	0.046	52
Silsesquioxane/MCPE	DPV	10.0	10.0	56
p-Phemodifed electrode	DPV	0.7	1.0	57
PANI/MnO_2-GCE	DPV	0.15	0.12	58
SPC electrode	SWV	0.05	0.05	59
(LDHf/GCE)	DPV	1.2	9.0	60
PASA/MWNTs/GCE	DPV	1.0	1.0	61
LRG/GCE	DPV	0.8	0.5	62
Poly(brilliant cresyl blue)/GCE	DPV	0.05	0.06	63
MWNT/GCE	DPV	0.20	0.75	64
TpBD-COF/ CPE	DPV	0.46	0.31	65
Po/DG6/MCPE	CV	0.09	0.11	35
Au/AB/GCE	CV	0.5	1.0	66
Flexible screen-printed carbon electrodes	DPV	0.82	0.12	67
Co@SnO_2–PANI/GCE	DPV	0.001578	0.00494	68
PtNiCu@FTO	CV, DPV	0.35	0.29	69
Poly-TZ/CTAB/MCPE	**CV**	**0.49**	**0.41**	**This work**

be: Ipa (10^{-5}A) = 0.48658 (C_0 mM L^{-1}) + 2.236, (r^2 = 0.99822). The detection limit for HQ at the poly-TZ/CTAB/MCPE was found to be 0.41 × 10^{-6} M, which is better than the reported detection limits for other modified electrodes and electrochemical methods listed in Table 2.[35,52,56–69]

3.11. The effect of solution pH variation on the oxidation of HQ at the poly-TZ/CTAB/MCPE

The electrochemical oxidation of 0.1 mM HQ at the poly-TZ/CTAB/MCPE was analyzed using cyclic voltammetry to investigate the effect of varying pH values. The findings, presented in Fig. S5,† indicate that the oxidation peak potentials shift towards a more negative side as the pH of the phosphate buffer solution increases from 5.5 to 8.0. The Epa *versus* pH graph, plotted in Fig. 3F, demonstrates a linear relationship between Epa and pH, with a linear regression equation of Epa (V) = 0.5360 − 0.0651 (pH), (r^2 = 0.9988). The value of the slope (0.0651 V/pH) implies the participation of an equal number of electrons and protons in the electrochemical reaction, in agreement with previous reports.[51,52,54]

3.12. Electrocatalytic oxidation of RC at the poly-TZ/CTAB/MCPE

The electrochemical behavior of 0.1 mM RC was investigated at the BCPE and poly-TZ/CTAB/MCPE in 0.2 M PBS of pH 7.4 using the CV technique with a scan rate of 0.05 V s^{-1}. The results, depicted in Fig. 4A, reveal that the sensitivity for RC detection at the BCPE was minimal, with an anodic peak potential at 0.6070 V. In contrast, the sensitivity for RC detection at the poly-TZ/CTAB/MCPE was significantly higher, with a lower oxidation potential at 0.5082 V. The electro-oxidations of RC at different electrode surfaces are shown in Fig. S6.† This suggests that the modified electrode could detect RC at physiological pH with an improved current response. Furthermore, the concentration of RC varied in the range of 0.05 mM to 0.45 mM at the poly-TZ/CTAB/MCPE, and the CV technique was used to investigate the influence of this variation. A good correlation between Ipa and the concentration of RC was obtained, as depicted in (Fig. S7 and S8†). A linear regression equation was derived as: Ipa (10^{-5}A) = 0.45953 (C_0 μM) + 1.1995, (r^2 = 0.99865). This indicates that this method could be helpful for the determination of RC in the aforesaid concentration range.

3.13. Simultaneous determination of CC, HQ and RC at the poly-TZ/CTAB/MCPE

The experiment aimed to simultaneously oxidize 0.5 mM CC, HQ, and RC at the poly-TZ/CTAB/MCPE surface, maintaining the solution pH at 7.4 and a scan rate of 0.05 V s^{-1}. Hence, the cyclic voltammograms were first recorded on the BCPE

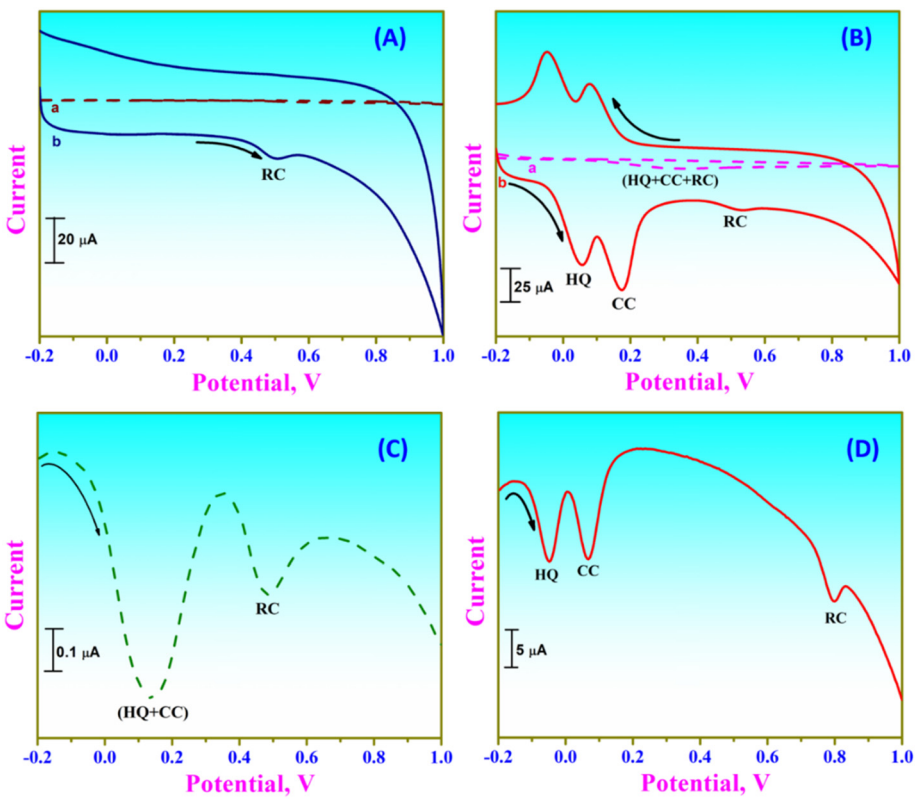

Fig. 4 (A) CV curves for 0.1 mM RC at BCPE (-----) and poly-TZ/CTAB/MCPE (—) in 0.2 M PBS of pH 7.4 at a scan rate of 0.05 V s^{-1}. (B) CV curves for determination of CC, HQ and RC in a ternary mixture – dashed line (at BCPE) and solid line (poly-TZ/CTAB/MCPE). (C) DPV curves for determination of CC, HQ and RC in a ternary mixture at BCPE (dashed line). (D) DPV curves for simultaneous determination and discrimination of a mixture of CC, HQ and RC (0.5 mM) at poly-TZ/CTAB/MCPE (solid line) at a scan rate of 0.05 V s^{-1}.

surface. It has been observed that the oxidation of these three molecules at the BCPE surface showed poor sensitivity and a low current signal, as indicated by the dashed line in Fig. 4B. The cyclic voltammogram at the bare CPE was broad-shaped and three signals are merged at a potential of 0.3547 V. However, the voltammogram obtained for the poly-TZ/CTAB/MCPE under identical conditions showed an elevated current signal with superior sensitivity. The anodic peaks could be distinguished, as illustrated by the solid line in Fig. 4B. The cyclic voltammetry technique yielded separate electroanalytical anodic peaks of CC, HQ, and RC at 0.1776 V, 0.0536 V, and 0.5304 V, respectively. The distance between the two peaks of CC and HQ was sufficient (0.1240 V) to distinguish and resolve CC and HQ in the presence of RC at the poly-TZ/CTAB/MCPE.

To affirm the above result, DPV was utilized owing to its high sensitivity and the absence of background current. A ternary mixture of 0.5 mM CC, HQ, and RC was subjected to DPV analysis at the surface of both the bare CPE and poly-TZ/CTAB/MCPE maintaining the same reaction conditions. At the bare CPE, the oxidation potentials of CC and HQ were not distinctly separated; instead, an overlapped anodic oxidation peak was observed at 0.137 V, and RC was detected at 0.487 V (Fig. 4C). However, the poly-TZ/CTAB/MCPE exhibited selective separation of the oxidation potentials of CC and HQ at 0.065 V and −0.051 V, respectively and the selective oxidation peak potential for RC was located at 0.799 V (Fig. 4D). In conclusion, the dihydroxy benzene isomers like CC, HQ, and RC can be simultaneously detected at the poly-TZ/CTAB/MCPE surface by using both CV and DPV techniques.

3.14. Interference study

Interference investigation was carried out at the poly-TZ/CTAB/MCPE by altering the concentration of one analyte while keeping the other constant in a binary mixture. The resulting data in Fig. 5A showed an increase in the peak current of CC with the increase of its concentration from 0.05 mM to 0.3 mM while keeping the concentration of HQ constant. Similarly, the variation of HQ concentration from 0.05 mM to 0.3 mM while keeping CC constant resulted in only an increase in the peak current of HQ, as shown in Fig. 5C. The linear relationship between peak current and concentration for both analytes was evident in the Fig. 5B and D. The corresponding linear regression equations can be written as below:

$$\mathrm{Ipa}(10^{-5}\ \mathrm{A}) = 1.06697(C_0\ \mu\mathrm{M\ L^{-1}}) + 7.9984,$$
$$(r^2 = 0.99593)(\text{for CC; HQ constant}).$$

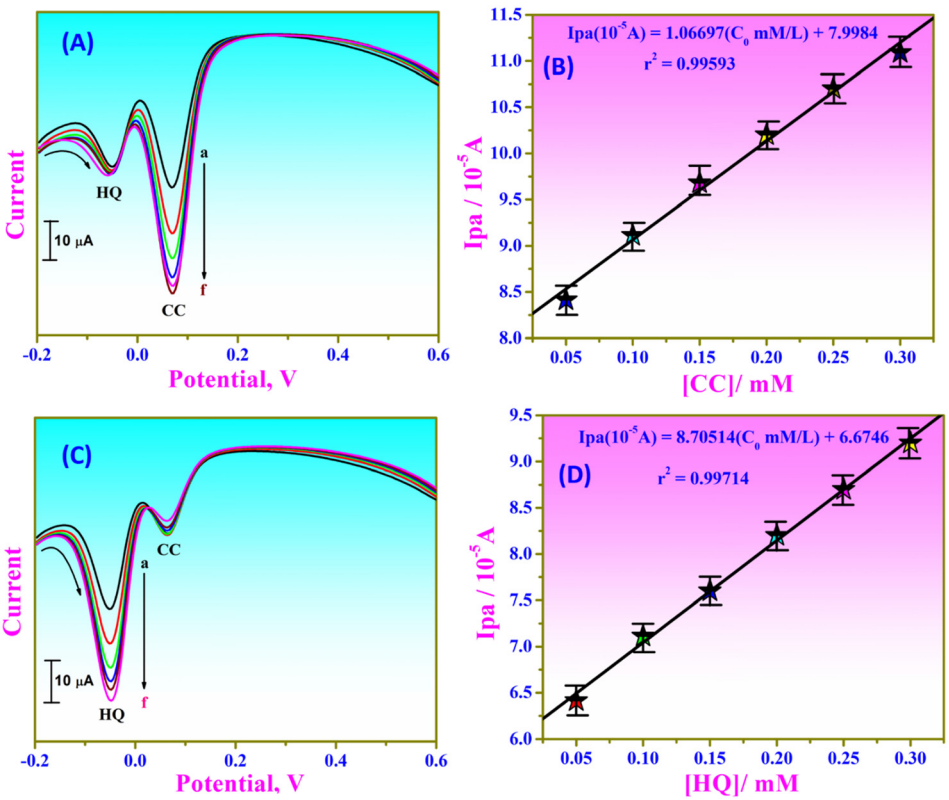

Fig. 5 (A) DPV curves of CC with different concentrations (a–f: 0.05 mM, 0.1 mM, 0.15 mM, 0.2 mM, 0.25 mM and 0.30 mM) in 0.2 M PBS of pH 7.4 in the presence of 0.05 mM HQ at poly-TZ/CTAB/MCPE. (B) Plot of anodic peak current *versus* concentration of [CC]. (C) DPV curves of HQ with different concentration (a–f: 0.05 mM, 0.1 mM, 0.15 mM, 0.2 mM, 0.25 mM and 0.30 mM) in 0.2 M PBS of pH 7.4 in presence of 0.05 mM CC at poly-TZ/CTAB/MCPE. (D) Plot of anodic peak current *versus* concentration of [HQ].

$$\text{Ipa}(10^{-5}\ \text{A}) = 8.70514(C_0\ \mu\text{M L}^{-1}) + 6.6746,\quad (r^2 = 0.99714)(\text{for HQ; CC constant}).$$

The results obtained in this study conclude that an accurate and interference-free determination of CC and HQ can be carried out at the newly developed poly-TZ/CTAB/MCPE surface. It can be noted from Fig. S9† that the addition of tenfold (0.5 mM) of different substances such as ascorbic acid, calcium chloride, dopamine, glucose, ammonium chloride, oxalic acid, paracetamol, starch, urea, and uric acid does not affect the determination of CC, HQ and RC at the poly-TZ/CTAB/MCPE. The change in current signal did not exceed 5.0%, reflecting the selectivity of the proposed electrode.

3.15. Real sample analysis

To evaluate the analytical performance of the fabricated sensor, it was applied to determine CC, HQ and RC in tap water. The results obtained are tabulated in Table 3 and it reflects a good analytical performance. The determination of CC, HQ and RC in the tap water sample was tested and the obtained results are tabulated in Table 3. When a known amount of CC was added to the tap water sample, a recovery of 97.2% to 101% was obtained. Similarly, when a known quantity of HQ was added to the tap water sample, a good recovery of 95.4% to 103.3% was observed. For RC, the recovery was 98.5% to 101%. Overall, these gathered results can be accepted and it reflects that the poly-TZ/CTAB/MCPE could be successfully applied for the determination of CC, HQ and RC in real samples without any interferences[70,71]

4. Conclusion

In the present work, we have developed an azo dye-surfactant-based electrochemical sensor capable of detecting dihydroxybenzene isomers in physiological pH of 7.4. The electrochemical analyses were done using CV and DPV techniques. The influences of change in concentration, scan rates and pH on electrocatalytic oxidations of the dihydroxy benzene isomers showed promising results with higher sensitivity and selectivity. Further, the fabricated electrode was used to separate CC, HQ and RC peaks using CV and DPV techniques. The LOD values obtained for CC, HQ and RC are better than the other reported values. Interference studies were carried out, and it has been observed that the isomers do not interfere with each other when present in a binary mixture. In addition, the synthesized sensor was effectively applied for the detection of dihydroxy benzene isomers in a tap water sample, with good recovery results. Hence, this new poly-TZ/CTAB/MCPE material can be applied to develop any sensing device for all three dihydroxy benzene isomers provided that the challenges are overcome with the help of scientists from multidisciplinary areas. The further scope of research to develop a technological device using this sensor lies ahead.

Table 3 Results obtained for CC, HQ and RC determination in the tap water sample at the poly-TZ/MCPE

Sample	Spiked	Found	Recovery (%)	SD ± RSD (%)
CC	1.0×10^{-6}	1.01×10^{-6}	101	0.0050 ± 0.0035
	3.0×10^{-6}	2.98×10^{-6}	99.3	0.0141 ± 0.0100
	5.0×10^{-6}	4.99×10^{-6}	99.8	0.0050 ± 0.0035
	7.0×10^{-6}	6.96×10^{-6}	99.4	0.0282 ± 0.0201
	9.0×10^{-6}	9.03×10^{-6}	100.3	0.0212 ± 0.0151
	1.1×10^{-5}	1.07×10^{-5}	97.2	0.0212 ± 0.0151
HQ	1.0×10^{-6}	1.02×10^{-6}	102	0.0141 ± 0.0100
	3.0×10^{-6}	2.97×10^{-6}	99.3	0.0148 ± 0.0105
	5.0×10^{-6}	4.98×10^{-6}	99.7	0.0106 ± 0.0075
	7.0×10^{-6}	7.06×10^{-6}	100.8	0.0424 ± 0.0303
	9.0×10^{-6}	9.03×10^{-6}	103.3	0.0212 ± 0.0151
	1.1×10^{-5}	1.105×10^{-5}	95.4	0.0353 ± 0.0252
RC	1.0×10^{-6}	0.99×10^{-6}	99	0.0050 ± 0.0035
	3.0×10^{-6}	3.03×10^{-6}	101	0.0212 ± 0.0151
	5.0×10^{-6}	4.96×10^{-6}	99.2	0.0282 ± 0.0201
	7.0×10^{-6}	6.90×10^{-6}	98.5	0.070 ± 0.050
	9.0×10^{-6}	8.97×10^{-6}	99.6	0.0212 ± 0.0151
	1.1×10^{-5}	1.109×10^{-5}	99	0.0050 ± 0.0035

Author contributions

Amit B. Teradale: conceptualization, data curation, formal analysis, investigation, methodology. Kailash S. Chadchan: methodology, investigation. Pattan-Siddappa Ganesh: resources, supervision, validation, visualization, data curation, writing – review & editing. Swastika. N. Das: conceptualization, resources, funding acquisition, writing-original draft, editing and project administration. Eno E. Ebenso: supervision, validation, visualization, writing – review & editing.

Conflicts of interest

The authors declare no conflict of interest, financial or otherwise.

Acknowledgements

We wish to express our gratitude to VGST (Vision Group of Science and Technology), Karnataka Science and Technology Promotion Society, Government of Karnataka, India, for funding the work [Ref. No: KSTePS/VGST-K-FIST L1/2018-19/GRD No.771/315. Dt. 17-07-2019]. Principal investigator: Dr. Swastika N. Das.

References

1 A. G. Calleley, C. F. Forster and D. A. Stafford, *Environ. Conserv.*, 1977, **6**(4), 328.
2 M. Buleandra, A. A. Rabinca, C. Mihailciuc, A. Balan, C. Nichita and I. Stamatin, *et al.*, *Sens. Actuators, B*, 2014, **203**, 824–832.
3 C. Bu, X. Liu, Y. Zhang, L. Li, X. Zhou and X. Lu, *et al.*, *Colloids Surf., B*, 2011, **88**(1), 292–296.
4 P. S. Ganesh and B. E. Kumara Swamy, *J. Mol. Liq.*, 2016, **220**, 208–215.
5 G. K. J. Chao and J. C. Suatoni, *J. Chromatogr. Sci.*, 1982, **20**(9), 436–440.

6 L. H. Wang and Y. P. Kuo, *Chromatographia*, 1999, **49**, 208–211.
7 B. L. Lee, H. Y. Ong, C. Y. Shi and C. N. Ong, *J. Chromatogr.*, 1993, **619**(2), 259–266, DOI: 10.1016/0378-4347(93)80115-K.
8 Y. G. Sun, H. Cui, Y. H. Li and X. Q. Lin, *Talanta*, 2000, **53**, 661–666.
9 P. Nagaraja, R. A. Vasantha and K. R. Sunitha, *J. Pharm. Biomed. Anal.*, 2001, **25**, 417–424.
10 M. F. Pistonesi, M. S. D. Nezio, M. E. Centurion, M. E. Palomeque, A. G. Lista and B. S. F. Band, *Talanta*, 2006, **69**, 1265–1268.
11 S. C. Moldoveanu and M. Kiser, *J. Chromatogr. A*, 2007, **1141**(1), 90–97.
12 S. Z. Mohammadi, H. Beitollahi, M. Safaei, Q. V. Le, H. W. Jang, M. Shokouhimehr and W. Peng, *Int. J. Electrochem. Sci.*, 2021, **16**, 2150565.
13 S. Tajik, H. Beitollahi, Q. V. Le, H. W. Jang, S. Y. Kim and K. Zhang, *et al.*, *RSC Adv.*, 2020, **10**(26), 15406–15429.
14 S. Tajik, H. Beitollahi, H. W. Jang and M. Shokouhimehr, *Talanta*, 2021, **232**, 122379.
15 F. GarkaniNejad, S. Tajik, H. Beitollahi and I. Sheikhshoaie, *Talanta*, 2021, **228**, 122075.
16 P. Mohammadzadeh Jahani, H. Beitollahi and S. Tajik, *Food Chem. Toxicol.*, 2022, **167**, 113274.
17 H. Beitollahi, S. Tajik, M. R. Aflatoonian and A. Makarem, *J. Electrochem. Sci. Eng.*, 2022, **12**(1), 199–208.
18 S. Tajik, H. Beitollahi, F. G. Nejad, K. Zhang, Q. V. Le and H. W. Jang, *et al.*, *Sensors*, 2020, **20**, 3364.
19 S. Z. Mohammadi, S. Tajik and H. Beitollahi, *J. Serb. Chem. Soc.*, 2019, **84**(9), 1005–1016.
20 K. S. Chadchan, A. B. Teradale, P. S. Ganesh and S. N. Das, *Mater. Chem. Phys.*, 2022, **290**, 126538.
21 P. Karami-Kolmoti, H. Beitollahi and S. Modiri, *Biomedicines*, 2023, **11**, 1869.
22 M. M. Foroughi, H. Beitollahi, S. Tajik, A. Akbari and R. Hosseinzadeh, *Int. J. Electrochem. Sci.*, 2014, **9**, 8407–8421.
23 M. R. Ganjali, H. Beitollahi, R. Zaimbashi, S. Tajik, M. Rezapour and B. Larijani, *Int. J. Electrochem. Sci.*, 2018, **13**, 2519–2529.
24 S. Z. Mohammadi, H. Beitollahi, M. Kaykhaii, N. Mohammadizadeh, S. Tajik and R. Hosseinzadeh, *Measurement*, 2020, **155**, 107522.
25 H. Beitollahi, S. Tajik, H. Parvan, H. Soltani, A. Akbari and M. H. Asadi, *Anal. Bioanal. Electrochem.*, 2014, **6**(1), 54–66.
26 B. Rajeswari, B. Sravani, M. Cheffena, R. J. Naik, Y. V. M. Reddy, G. Madhavi, K. V. N. S. Reddy and M. J. Kim, *Inorg. Chem. Commun.*, 2023, **151**, 110627; S. Tajik, N. Akbarzadeh-Torbati, M. Safaei and H. Beitollahi, *Int. J. Electrochem. Sci.*, 2019, **14**(5), 4361–4370.
27 S. Tajik, F. Sharifi and H. Beitollahi, *Ind. Eng. Chem. Res.*, 2023, **62**(11), 4694–4703.
28 P. M. Mohammadzadeh Jahani, M. Jafari, V. K. Gupta and S. Agarwal, *Int. J. Electrochem. Sci.*, 2020, **15**(1), 947–958.
29 S. Tajik, H. Beitollahi, Z. Dourandish, K. Zhang, Q. V. Le, T. P. Nguyen, S. Y. Kim and M. Shokouhimehr, *Sensors*, 2020, **20**(13), 3675.
30 E. J. Nixon, R. Sakthivel, Z. A. ALOthman, P. S. Ganesh and R. J. Chung, *Food Chemistry*, 2023, **409**, 135324.
31 S. Tajik, H. Beitollahi, S. Z. Mohammadi, M. Azimzadeh, K. Zhange, Q. V. Le, Y. Yamauchi, H. W. Jang and M. Shokouhimehr, *RSC Adv.*, 2020, **10**, 30481–30498.
32 F. Chang, H. Wang, S. He, Y. Gu, W. Zhu and T. Li, *RSC Adv.*, 2021, **11**, 31950.
33 J. Tashkhourian, M. Daneshi, F. Nami-Ana, M. Behbahani and A. Bagheri, *J. Hazard. Mater.*, 2016, **318**, 117–124.
34 T. Zhou, W. Gao, Y. Gao and Q. Wang, *J. Electrochem. Soc.*, 2019, **166**(12), B1069–B1078.
35 K. Chetankumar, B. E. Kumara Swamy and S. C. Sharma, *et al.*, *Sci. Rep.*, 2021, **11**, 15064.
36 A. B. Teradale, S. D. Lamani, P. S. Ganesh, B. E. Kumara Swamy and S. N. Das, *Anal. Bioanal. Electrochem.*, 2019, **11**(9), 1176–1190.
37 C. B. A. Hassine, H. Kahri and H. Barhoumi, *IEEE Sens. J.*, 2021, **21**(17), 18864–18870.
38 J. Yu, W. Du, F. Zhao and B. Zeng, *Electrochim. Acta*, 2009, **54**(3), 984–988.
39 W. Liu, L. Wu, X. Zhang and J. Chen, *Bull. Korean Chem. Soc.*, 2014, **35**(1), 204–210.
40 Z. Wang, S. Li and Q. Lv, *Sens. Actuators, B*, 2007, **127**(2), 420–425.
41 D. Zhang, Y. Peng, H. Qi, Q. Gao and C. Zhang, *Sens. Actuators, B*, 2009, **136**(1), 113–121.
42 H. Yin, Q. Zhang, Y. Zhou, Q. Ma, T. Liu, L. Zhu and S. Ai, *Electrochim. Acta*, 2011, **56**, 2748–2753.
43 M. Aragó, C. Ariño, À. Dago, J. M. Díaz-Cruz and M. Esteban, *Talanta*, 2016, **160**, 138–143.
44 T. C. Canevari, L. T. Arenas, R. Landers, R. Custodio and Y. Gushikem, *Analyst*, 2013, **138**(1), 315–324.
45 M. U. Hossain, M. T. Rahman and M. Q. Ehsan, *Int. J. Anal. Chem.*, 2015, **2015**, 862979.
46 A. B. Teradale, S. D. Lamani, P. S. Ganesh, B. E. Kumara Swamy and S. N. Das, *Anal. Chem. Lett.*, 2017, **7**(6), 748–764.
47 A. B. Teradale, S. D. Lamani, P. S. Ganesh, B. E. Kumara Swamy and S. N. Das, *Z. Phys. Chem.*, 2018, **232**, 345–358.
48 M. Ghalkhani, N. Zare, F. Karimi, C. Karaman, M. Alizadeh and Y. Vasseghian, *Food Chem. Toxicol.*, 2022, **161**, 112830.
49 H. Karimi-Maleh, H. Beitollahi, P. S. Kumar, S. Tajik and P. M. Jahani, *et al.*, *Food Chem. Toxicol.*, 2022, **164**, 112961.
50 E. Forgacs, T. Cserháti and G. Oros, *Environ. Int.*, 2004, **30**(7), 953–971.
51 P. S. Ganesh and B. E. K. Swamy, *J. Electroanal. Chem.*, 2015, **756**, 193–200.
52 A. B. Teradale, S. D. Lamani, P. S. Ganesh, B. E. K. Swamy and S. N. Das, *Anal. Bioanal. Electrochem.*, 2019, **11**(9), 1176–1190.
53 A. B. Teradale, S. D. Lamani, P. S. Ganesh, B. E. K. Swamy and S. N. Das, *Sens. Bio-Sens. Res.*, 2017, **15**, 53–59.
54 A. B. Teradale, S. D. Lamani, B. E. K. Swamy, P. S. Ganesh and S. N. Das, *Adv. Phys. Chem.*, 2016, **2016**, 8092860.
55 A. J. Bard and L. R. Faulkner, *Electrochemical Methods Fundamentals and Applications*, John Wiley and Sons, 2nd edn, 2001, DOI: 10.1023/A:1021637209564.

56 P. S. Da-Silva, B. C. Gasparini, H. A. Magosso and A. Spinelli, *J. Braz. Chem. Soc.*, 2013, **24**(4), 695–699.

57 L. Wang, *et al.*, *Int. J. Electrochem. Sci.*, 2006, **1**, 403–413.

58 M. U. A. Prathapa, B. Satpati and R. Srivastava, *Sens. Actuators, B*, 2013, **186**, 67–77.

59 S. M. Wang, W. Y. Su and S. H. Cheng, *Int. J. Electrochem. Sci.*, 2010, **5**, 1649–1664.

60 M. Li, F. Ni, Y. Wang, S. Xu, D. Zhang, S. Chen and L. Wang, *Electroanalysis*, 2009, **21**, 1521–1526.

61 D. M. Zhao, X. H. Zhang, L. J. Feng, L. Jia and S. F. Wang, *Colloids Surf.*, 2009, **74**(1), 317–321.

62 T. Lai, W. Cai, W. Dai and J. Ye, *Electrochim. Acta*, 2014, **138**, 48–55.

63 A. A. Shaikh, S. K. Saha, P. K. Bakshi, A. Hussain and A. J. S. Ahammad, *J. Electrochem. Soc.*, 2013, **160**, B37–B42.

64 H. Qi and C. Zhang, *Electroanalysis*, 2005, **17**, 832–838.

65 Y. Xin, N. Wang, C. Wang, W. Gao, M. Chen, N. Liu, J. Duan and B. Hou, *J. Electroanal. Chem.*, 2020, **877**, 114530.

66 X. Zhu, M. Wang, C. Xu and S. Shi, *ChemSelect*, 2021, **6**(34), 8565–8569.

67 A. C. Sá, S. C. Barbosa, P. A. Raymundo-Pereira, D. Wilson, F. M. Shimizu, M. Raposo and O. N. Oliveira, Jr, *Chemosensors*, 2020, **8**(4), 103.

68 Q. Saleem, S. Shahid, M. Javed, S. Iqbal, A. Rahim, S. Mansoor, A. Bahadur, N. S. Awwad, H. A. Ibrahium, R. S. Almufarij and E. B. Elkaeed, *RSC Adv.*, 2023, **13**, 10017–10028.

69 M. Arsalan, X. Qiao, A. Awais, Y. Wang, S. Yang, Q. Sheng and T. Yue, *Electroanalysis*, 2021, **33**, 1528–1538.

70 P. S. Ganesh, B. E. K. Kumara Swamy, O. E. Fayemi, E. M. Sherif and E. E. Ebenso, *Sens. Bio-Sens. Res.*, 2018, **20**, 47–54.

71 Y. V. M. Reddy, J. H. Shin, V. N. Palakollu, B. Sravani, C.-H. Choi, K. Park, S.-K. Kim, G. Madhavi, J. P. Park and N. P. Shetti, *Adv. Colloid Interface Sci.*, 2022, **304**, 102664.